Theor Chim Acta (1996) 93: 1–16

Theoretica Chimica Acta

Diagrammatic valence bond studies on hemocyanin

Pravat Kumar Mandal[1], **P. T. Manoharan**[1], **Bhabadyuti Sinha**[2], **S. Ramasesha**[2,3]

[1] Department of Chemistry, Indian Institute of Technology, Madras 600036, India

[2] Solid State and Structural Chemistry Unit, Indian Institute of Science, Bangalore 560012, India

[3] Jawaharlal Nehru Center for Advanced Scientific Research, Indian Institute of Science Campus, Bangalore 560012, India

Received June 2, 1995/Accepted June 2, 1995

Summary. The Diagrammatic Valence Bond studies on the active sites of hemocyanin, consisting of two Cu(I) ions and an oxygen molecule, are performed to find out the stable geometrical pattern and electronic structure. Different parameters used in this theoretical approach are taken from existing literature on high T_c superconductors. Attempts have been made to find out the differences in electronic structure of $[Cu_2O_2]^{+2}$ and $[Cu_2O_2N_4]^{+2}$ as it is observed that coordination of nitrogen ligand do affect electronic structure i.e. spin excitation gaps and charge and spin density distribution. A comparison of our results with earlier theoretical results are also presented.

Key words: DVB theory – Active site – Hemocyanine – Charge density – Spin density – Excitation gap

1 Introduction

Hemocyanin is a large, non-hame, copper containing protein which occurs in hemolymph of many invertebrate species. It is mainly found in two phylla, namely, molluscan and arthropodan, which have different quaternary structure and copper–protein ratio. Arthropodan hemocyanin consists of hexamers or multihexamers with subunits of molecular weight (MW) 75,000 while the molluscan hemocyanin is a cylindrical oligomer [1–3] with subunits of molecular weight $\approx$ 400,000. It reversibly binds dioxygen and acts as a dioxygen transport protein. The deoxy form is colourless while the oxy form is blue coloured and rich in electronic spectra.

The spectral features associated with the oxyhemocyanin active site are quite unusual compared to known inorganic copper complexes [4]. In particular, while the copper is believed to be divalent in the oxyprotein, no EPR signal could be observed. This is explained by strong magnetic coupling between the coppers and susceptibility measurements [5] using high sensitivity SQUID have allowed a lower limit to be placed on antiferromagnetic exchange interactions of 550 cm^{-1}. The active site of hemocyanin has been thoroughly studied by different spectroscopic techniques such as Resonance Raman (RR), UV, Electron Spin Resonance (ESR) and Extended X-ray Absorption Fine Structure (EXAFS). The O–O stretch-

ing at 744–749 cm^{-1} obtained from RR studies [6] on oxyhemocyanin clearly indicates the possibility of peroxo form of the dioxygen and electron transfer from the Cu(I) to the oxygen atom. The UV-Visible spectra [7, 8] exhibit an absorption band in the 500–600 nm range, which could be assigned to an $O_2^{2-} \rightarrow Cu(II)$ charge transfer absorption. The Cu ... Cu separation [9] of oxyhemocyanin is close to 3.6 Å. A recent crystal structure on hemocyanin indicates that three imidazoles of histidine residues are attached to each copper in hemocyanin [10, 11]. However, since the crystal structure of oxyhemocyanin is not available till date the questions on binding of O_2 with copper and the preferred geometry of the active site as a whole remains to be answered satisfactorily. Therefore, the stress has recently been on the preparation of some model compounds which could mimic the properties of oxyhemocyanin.

Karlin et al. [12] first synthesized the peroxo dinuclear copper complex from dinucleating ligand containing a bridging phenoxo group and it was also shown that the complex reacts with oxygen quasireversibly. Another peroxo dinuclear complex which has the characteristics of mimicing oxyhemocyanin was also reported by Kitajima et al. [13, 14] and Fenton et al. [15, 16]. These peroxo complexes do not contain a bridging ligand other than the peroxide ion and they exhibit some remarkable characteristics such as diamagnetism, ν (O–O) stretching frequencies at 725–760 cm^{-1}, a symmetrical coordination mode of the peroxide ion as found in oxy-He as established by Resonance Raman spectroscopy, characteristic absorption bands appearing at $\simeq$ 350 nm (ε, 20,000) and $\simeq$ 150 nm (ε, 1000), absence of the resonance band assignable to Cu–O stretching vibration with 514.5 nm excitation and Cu–Cu separation of 3.6 Å, etc.

Theoretically, a few attempts have been already made to understand the geometrical pattern of oxygen molecule in the active site ($[Cu_2O_2]^{+2}$) of oxyhemocyanin molecule. Solomon et al. [17–19] have reported a spin-unrestricted SCF-Xα-Scattered wave (SCF-Xα-SW) calculation on peroxide-bridged copper dimer which has relevance to hemocyanin. They have considered two geometrical forms i.e. end-on-*cis*-μ-1,2 peroxo and side-on-μ-η^2-peroxo. The singlet–triplet energy gap was found to be 1850 cm^{-1} and 5660 cm^{-1} which are far away from the experimental findings. Maddaluno et al. [20] have carried out non-empirical calculations for all possible geometrical patterns of $[Cu_2O_2]^{+2}$. They have considered four different configurations namely μ-monoxo, *cis*-μ-dioxo, *trans*-μ-dioxo and $\eta^2 : \eta^2$. In their formulation, only bare copper atoms and oxygen molecule were considered. They calculated the singlet–triplet energy gap for all the geometries and charge densities on oxygen atoms. It has been assumed by Maddaluno *et al.* [20] that addition of nitrogen ligand to copper atoms will not affect spin excitation gap of the $[Cu_2O_2]^{+2}$; but Chandler and Manoharan [21] have proved the importance of nitrogen ligand by density functional studies on hemocyanin. It was found that inclusion of nitrogen atoms has an effect on singlet–triplet energy gap.

From earlier theoretical works by Mandal et al. [22, 23] on exchange coupled copper(II) dimers we found that coordination of nitrogen atoms with copper do affect the spin excitation energy gap. We thought it worthwhile to extend the same theoretical approach for an understanding of the active site of hemocyanin. In this new theoretical approach different parameters like site energy, different exchange integrals were taken from existing literature based on high T_c superconductors [24–26]. Our objective is to decipher the detailed electronic structure of $[Cu_2O_2]^{+2}$ with different geometrical pattern of the oxygen molecule. The effect of adding nitrogen ligands to $[Cu_2O_2]^{+2}$ and thereby determining the electronic structure of $[Cu_2O_2N_4]^{+2}$ have also been discussed.

2 Model Hamiltonian and computational details

We have included in our study all five of the 3*d* orbitals on copper atoms, the three 2*p* orbitals of the oxygen atoms and nitrogen orbital containing the lone pair involved in bonding with copper atom (whenever nitrogen atoms are considered) have been considered. Thus, if we are dealing with $[Cu_2O_2]^{+2}$, we have 28 electrons in 16 orbitals and in the $[Cu_2O_2N_4]^{+2}$ case we have 36 electrons in 20 orbitals. We have considered four different geometries for $[Cu_2O_2N_4]^{+2}$ as shown in Fig. 1 and the same geometries without nitrogen ligands were used for calculating the electronic structure of $[Cu_2O_2]^{+2}$. In order to compare different geometries wherein the symmetries are widely different, there msut be a consistent parameterization scheme. Depending upon the relative positions of the oxygen and copper atoms, the sign and magnitude of the one-electron transfer integral between a pair of orbitals could vary widely. Therefore, we have used a scheme in which the one-electron integrals between the various orbitals for different geometries are assumed to be proportional to the corresponding overlap integral. The overlap integral have been obtained by locating a Gaussian $\exp(-\alpha r^2)$, with $\alpha = 1$, on each of the atoms in the chosen pair and having the desired angular geometry (e.g. $d_{x^2-y^2}$, p_x, etc.). The transfer integral between the $d_{x^2-y^2}$ orbital of Cu and p_x orbital of oxygen, at an internuclear separation of 1.95 Å in the σ-bonding geometry, is taken to be 1.3 eV from literature that now exist for the Cu and oxygen parameters realized from studies on high T_c superconductor containing CuO_2 layer [24–26]. The overlap integral between these orbitals at this distance is $s_0 = 0.143368$. Given the overlap integrals between a *d–p* pair, the transfer integral is now taken to be 1.3 (s/s_0) eV.

The *d–p* transfer integrals involving the Cu and O orbitals for various geometries are given in Tables 1–4. The sign of the transfer integral is taken to be opposite to that of the overlap integral. This approach has been employed for the Cu–O transfer integrals. The inter-oxygen transfer between the various 2*p*-orbitals has been taken to be of two kinds, the σ-type of transfer and π type transfer, the earlier

Table 1. Transfer integrals in eV for geometry I. Orbitals (1–5) and (12–16) correspond to the d_{xy}, d_{xz}, d_{yz}, d_{z^2} and $d_{x^2-y^2}$ orbitals on the copper atoms 1 and 2, respectively. Orbitals 6–8 and 9–11 refers to p_x, p_y, p_z orbitals on oxygen atoms 1 and 2, respectively. (...) indicates zero transfer integral

j ⇒	6	7	8	9	10	11
i ⇓	p_x^{I}	p_y^{I}	p_z^{I}	p_x^{II}	p_y^{II}	p_z^{II}
1. d_{xy}^{I}	1.246	−0.404	...	1.246	0.404	...
2. d_{xz}^{I}	0.202	0.603	...	−0.202	0.623	...
3. d_{yz}^{I}	...	...	0.623	...	...	0.623
4. $d_{z^2}^{\mathrm{I}}$	...	...	0.202	...	...	−0.202
5. $d_{x^2-y^2}^{\mathrm{I}}$	0.623	0.202	...	0.623	−0.202	...
12. d_{xy}^{II}	1.246	0.404	...	1.246	−0.404	...
13. d_{xz}^{II}	−0.202	0.603	...	0.202	0.623	...
14. d_{yz}^{II}	...	...	0.623	...	...	0.623
15. $d_{z^2}^{\mathrm{II}}$	...	...	−0.202	...	...	0.202
16. $d_{x^2-y^2}^{\mathrm{II}}$	0.623	−0.202	...	0.623	0.202	...

Table 2. Transfer integrals in eV for geometry II. Orbitals numbering is as in Table 1

⋱ j⇒	6	7	8	9	10	11
i⇓	p_x^{I}	p_y^{I}	p_z^{I}	p_x^{II}	p_y^{II}	p_z^{II}
1. d_{xy}^{I}	0.829	⋯	⋯	0.177	⋯	⋯
2. d_{xz}^{I}	⋯	0.415	⋯	⋯	0.088	⋯
3. d_{yz}^{I}	0.498	⋯	0.416	0.054	⋯	0.088
4. $d_{z^2}^{\mathrm{I}}$	⋯	0.498	⋯	⋯	0.054	⋯
5. $d_{x^2-y^2}^{\mathrm{I}}$	0.415	⋯	1.493	0.088	⋯	0.162
12. d_{xy}^{II}	−0.177	⋯	⋯	−0.829	⋯	⋯
13. d_{xz}^{II}	⋯	−0.088	⋯	⋯	−0.415	⋯
14. d_{yz}^{II}	0.054	⋯	−0.088	0.498	⋯	−0.416
15. $d_{z^2}^{\mathrm{II}}$	⋯	0.054	⋯	⋯	0.498	⋯
16. $d_{x^2-y^2}^{\mathrm{II}}$	−0.088	⋯	0.162	−0.415	⋯	1.493

Table 3. Transfer integrals in eV for geometry III. Orbitals numbering is as in Table 1

⋱ j⇒	6	7	8	9	10	11
i⇓	p_x^{I}	p_y^{I}	p_z^{I}	p_x^{II}	p_y^{II}	p_z^{II}
1. d_{xy}^{I}	1.221	−0.396	⋯	1.221	0.396	⋯
2. d_{xz}^{I}	0.125	0.537	−0.073	−0.125	0.684	0.073
3. d_{yz}^{I}	−0.007	−0.073	0.537	0.140	0.073	0.684
4. $d_{z^2}^{\mathrm{I}}$	−0.073	−0.007	0.125	0.073	0.140	−0.125
5. $d_{x^2-y^2}^{\mathrm{I}}$	0.537	0.125	0.125	0.684	−0.125	0.271
12. d_{xy}^{II}	1.221	0.396	⋯	1.221	−0.396	⋯
13. d_{xz}^{II}	−0.271	0.537	−0.073	0.271	0.684	0.073
14. d_{yz}^{II}	−0.140	−0.073	0.537	0.007	0.073	0.684
15. $d_{z^2}^{\mathrm{II}}$	−0.073	−0.140	−0.271	0.073	0.007	0.271
16. $d_{x^2-y^2}^{\mathrm{II}}$	0.537	−0.271	−0.271	0.684	0.271	−0.125

having a value of (− 7.0 eV) larger than that for the latter (− 3.5 eV). Symmetry precludes any electron transfer between the σ-orbital on one oxygen and the π-orbital on another. The Cu–N transfer integral is assumed to be only between the d_{xy} orbital on the copper atom and the sp^3 hybrid orbital on the nitrogen site and taken to be 1.4 eV. This is slightly larger than the standard Cu–O transfer integral and accounts for the more diffused p-orbital on the nitrogen atoms. The transfer integral between the nitrogen orbitals and all other orbitals in the system are neglected. So also are the direct transfer integrals between the two copper sites. The diagonal part of the one-electron Hamiltonian corresponds to the orbital energies. We have taken the orbital energy of Cu to be zero and the oxygen p-orbital have an orbital energy of − 4.0 eV and the nitrogen sp^3 lone-pair orbital have an orbital energy − 12.0 eV based on previous studies.

The two-electron integrals in the Hamiltonian are dealt within the ZDO approximation, so that any integral involving an overlap charge cloud is neglected.

Table 4. Transfer integrals in eV for geometry IV. Orbitals numbering is as in Table 1

i ⇓ j ⇒	6	7	8	9	10	11
	p_x^{I}	p_y^{I}	p_z^{I}	p_x^{II}	p_y^{II}	p_z^{II}
1. d_{xy}^{I}	0.726	⋯	⋯	0.083	⋯	⋯
2. d_{xz}^{I}	⋯	0.363	⋯	⋯	0.042	⋯
3. d_{yz}^{I}	0.235	⋯	0.363	0.054	⋯	0.042
4. $d_{z^2}^{\mathrm{I}}$	⋯	0.235	⋯	⋯	0.054	⋯
5. $d_{x^2-y^2}^{\mathrm{I}}$	0.363	⋯	0.706	0.042	⋯	0.163
12. d_{xy}^{II}	−0.726	⋯	⋯	−0.083	⋯	⋯
13. d_{xz}^{II}	0.235	−0.363	⋯	⋯	−0.042	⋯
14. d_{yz}^{II}	0.235	⋯	−0.363	0.054	⋯	−0.042
15. $d_{z^2}^{\mathrm{II}}$	⋯	0.235	⋯	⋯	0.054	⋯
16. $d_{x^2-y^2}^{\mathrm{II}}$	−0.363	⋯	0.706	−0.042	⋯	0.163

The inter-atom two electron integrals are further parametrized using Ohno parameterization [27] wherein, the repulsion between an electron in orbital i on atom A and orbital j on atom B, namely $\langle i_A i_A \,|\, j_B j_B \rangle$ denoted as V_{i_A, j_B} is to be taken

$$V_{i_A,j_B} = 14.397\left[\left(\frac{28.794}{(U_i + U_j)}\right)^2 + r_{AB}^2\right]^{-1/2}, \tag{1}$$

where U_A is the integral $\langle i_A i_A \,|\, i_A i_A \rangle$ and r_{AB} is the distance between the two centers A and B. Besides the ZDO approximation [28], we have also ignored integrals of the type $\langle i_A i'_A \,|\, j_A j'_A \rangle$, for $i_A \neq i'_A$ or $j_A \neq j'_A$. This is tantamount to neglecting the repulsion between electrons where any one of the electrons is in a mixed charge cloud on any site and this goes beyond the inter-site ZDO approximation. The neglect of this type of interaction integral is justified as they are expected to be an order of magnitude smaller than the integral $\langle i_A i_A \,|\, j_A j_A \rangle$. The on-site two electron integrals retained, besides the one representing repulsion between electrons in the same orbital (U_A), are integrals of the type $\langle i_A i_A \,|\, j_A j_A \rangle$ designated as U_{AA}. Here again we neglect integrals of the type $\langle i_A j_A \,|\, k_A l_A \rangle$. For $i_A \neq j_A$, $k_A \neq l_A$. The only other on-site two electron integral retained is the direct exchange integral $K_A = \langle i_A j_A \,|\, j_A i_A \rangle$ without which Hund's rule on an atom does not exist. To summarize we retain two-electron integrals on a given site of the type U_A, U_{AA} and K_A and these integrals are further assumed to be the same for all orbitals in the given manifold on a given atom.

The Hamiltonian developed by Pople et al. and Pariser et al. [28, 29] with these parameterization can be written as

$$H = H_{\mathrm{tr}} + H_{\mathrm{int}}, \tag{2}$$

where H_{tr} is given by

$$H_{\mathrm{tr}} = \sum_{\langle ij \rangle} t_{ij}(a_{i\sigma}^{\dagger} a_{j\sigma} + \mathrm{h.c}) + \sum_i \varepsilon_i \hat{n}_i, \tag{3}$$

where, the transfer integrals, t_{ij} for different geometries are given in Tables 1–4. $a_{i\sigma}^{\dagger}$ ($a_{i\sigma}$) creates (annihilates) an electron in the ith orbital with spin σ. ε_i is the site

Table 5. Electron repulsion integrals U_A, U_{AA} and orbital energies for Cu, O and N atoms in units of eV

Atom	U_A	U_{AA}	ε
Cu	10.5	6.0	0.00
O	6.0	4.0	− 4.05
N	15.0	···	− 12.00

Table 6. Complete Hilbert space dimensionalities of various spin space in the $[Cu_2O_2]^{+2}$ and $[Cu_2O_2N_4]^{+2}$ systems

	$[Cu_2O_2]^{+2}$	$[Cu_2O_2N_4]^{+2}$
Singlet	5440	13300
Triplet	7140	17955
Quintet	1820	4845

energy of the ith orbital and $\hat{n}_i$ is the occupation number operator of the ith orbital. $\langle ij \rangle$ runs over the pairs of orbitals of nearest neighbour copper and oxygen and copper and nitrogen.

H_{int} is given by

$$H_{\text{int}} = \frac{1}{2}\sum_{ij} \langle ii \,|\, jj \rangle [\hat{E}_{ii}\hat{E}_{jj} - \delta_{ij}\hat{E}_{ij}] + \sum_{i>j} \langle ij \,|\, ji \rangle [\hat{E}_{ij}\hat{E}_{ji} - \hat{E}_{ii}] \tag{4}$$

with $\hat{E}_{ij} = \sum_\sigma a^\dagger_{i\sigma} a_{j\sigma}$ in the first summation, orbitals i and j could be on the same atom or on different atoms. In the second summation, however, the orbitals i and j are restricted to the same atom. The parameters for two-electron integrals and the site energies are given in Table 5. We have carried out calculations for many parameter sets within a small range of variations but reported results are on one set of parameters as the results of our calculations vary only slightly over this parameter set.

The exact low-lying eigenvalues and eigenfunctions of the model Hamiltonian are obtained for different spin states using a second quantised Valence Bond (VB) approach which has been recently reviewed [31]. The eigenvalues and eigenfunctions are exact since the model spans a finite dimensional Hilbert space (Table 6) and an exact representation of the Hamiltonian in matrix form is obtained in this complete finite dimensional basis. For each geometry, besides energies of low-lying states in different spin spaces, we have computed the charge density distribution and in the high-spin states, the spin densities at different sites. The novel feature of the calculations in this context is that in the interaction part of the Hamiltonian, the exchange term leads to both diagonal and off-diagonal matrix elements. In Pariser–Parr–Pople (PPP) type of Hamiltonian [28, 29] for which VB theory has been widely applied, the VB diagrams are eigenfunctions of the interaction part of the Hamiltonian (H_{int}). To handle this new feature, a set of VB rules for the operation of exchange operator on a VB diagram were derived. The off-diagonal matrix element arises since the exchange operator operating on a VB state with two electrons in one of the degenerate orbitals and none in another on the same atom

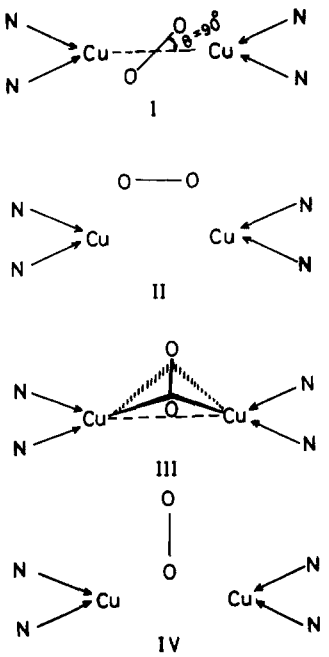

Fig. 1. Different geometrical patterns of the active sites of hemocyanin for calculating their electronic structure. Cu–Cu distance is 3.7 Å; Cu–N and O–O bond distances are 1.90 Å and 1.20 Å, respectively

interchanges the occupancies through a double hop. The setting up the Hamiltonian matrix is similar to previous applications [31, 32]. As the VB basis is nonorthogonal the Hamiltonian matrix is nonsymmetric. A few long-lying eigenvalues of the nonsymmetric matrix can be obtained by the usual small matrix techniques [33].

3 Results and discussion

We have carried out the multi-band extended Hubbard calculations [34–36] on four different geometries of $[Cu_2O_2]^{+2}$ as well as $[Cu_2O_2N_4]^{+2}$ as shown in Fig. 1. While dealing with different spin state energies, our past experience has shown that the critical parameter to which the energy level ordering of the different spin states is sensitive to the direct exchange integral between degenerate orbitals on the same site investigated [23, 30]. Hence, we have concentrated almost exclusively on the variation in the different properties corresponding to these geometries, as a function of the direct exchange integrals K_d and K_p of the d-orbitals of copper and the p-orbitals of oxygen. Subject to these constraints, we report results on the spin excitation gaps, the charge densities and the spin densities for the four geometries at different sites as a function of direct exchange integral.

3.1 $[Cu_2O_2]^{+2}$ *system*

In Table 7, the energies of the lowest two states for the singlet, triplet and the quintet states are given in different geometries for three values of $K_d = K_p = K$.

Table 7. Energies in units of cm^{-1} of low-lying states in the four different geometries for the $(Cu_2O_2)^{+2}$ system for different values of the exchange integral K ($= K_p = K_d$) in eV. All the energies are referred to the lowest singlet state for the specified geometry and K. Negative energies imply the state to be more stable than the lowest singlet state

		K (eV)		
Geometry	Spin state	0.04	0.10	0.20
I	S_1	0	0	0
	S_2	1395	645	2433
	T_1	971	− 169	− 913
	T_2	18437	16421	15742
	Q_1	59768	59328	60187
	Q_2	61228	60202	61615
II	S_1	0	0	0
	S_2	3183	9380	8636
	T_1	1540	− 4500	− 9050
	T_2	2981	4927	439
	Q_1	9982	79598	75348
	Q_2	10072	80497	76267
III	S_1	0	0	0
	S_2	1145	620	1382
	T_1	726	− 460	− 1597
	T_2	18200	20409	19346
	Q_1	57988	62811	63324
	Q_2	59237	63541	64541
IV	S_1	0	0	0
	S_2	11551	11196	1011
	T_1	− 1746	− 4371	− 8861
	T_2	9907	7220	4174
	Q_1	42729	40724	36882
	Q_2	43110	40615	36881

The energy value zero in Table 7 is referred to the lowest singlet state in any given geometry. We note that for a K value of 0.04 eV, the ground state is a singlet in the first three geometries but triplet in the fourth geometry. When the K value increases, the triplet becomes the ground state in all geometries. The quintet state is well above the low-lying singlets and triplets. In the first three geometries wherein the ground states are singlets, the singlet–triplet energy gap is the smallest in geometry-III (0.090 eV) and largest in the second geometry (0.191 eV) with the gap in the first geometry being intermediate (0.120 eV). The singlet–singlet energy gaps are less than 0.4 eV in the first three geometries but is large in the fourth geometry. The triplet–triplet energy gaps are larger in the fourth geometry. The triplet–triplet energy gaps are greater than 1 eV in all geometries except in the second. The quintet–quintet energy gaps are all rather small although the lowest quintet itself is a rather high-energy state.

In Table 8 we have shown the charge and spin density distribution in this system. In all geometries excepting the second, the copper ion is almost in d^{10} configuration and there is very little charge transfer to the oxygen atoms. In the

Table 8. Charge densities and spin densities for $S > 0$ at the copper and oxygen sites of the $[Cu_2O_2]^{+2}$ system in the lowest state of different spin subspaces and geometries for $K\ (= K_p = K_d) = 0.04$ eV and 0.1 eV. O^U and O^L refer to upper and lower oxygen atoms in geometry IV.

Geometry	Atom	Charge density			Spin density	
		Singlet	Triplet	Quintet	Triplet	Quintet
$K = 0.04$ eV						
I	Cu	9.759	9.856	9.252	0.116	0.739
	O	4.239	4.143	4.739	0.883	1.261
II	Cu	8.839	8.732	8.355	0.902	1.644
	O	5.161	5.268	5.645	0.099	0.356
III	Cu	9.766	9.854	9.251	0.107	0.745
	O	4.234	4.146	4.749	0.892	1.264
IV	Cu	9.935	9.769	9.399	0.033	0.597
	O^U	2.326	2.636	3.312	1.894	2.677
	O^L	5.805	5.826	5.871	0.041	0.128
$K = 0.1$ eV						
I	Cu	9.850	9.880	9.360	0.090	0.630
	O	4.140	4.090	4.630	0.910	1.340
II	Cu	8.930	8.790	8.350	0.980	1.640
	O	5.060	5.200	5.640	0.110	0.360
III	Cu	9.780	9.860	9.300	0.080	0.620
	O	4.210	4.120	4.690	0.920	1.370
IV	Cu	9.950	9.920	9.450	0.020	0.540
	O^U	2.290	2.280	3.190	1.940	2.790
	O^L	5.810	5.810	5.870	0.039	0.120

nonzero spin states, the spin density almost exclusively resides on the oxygen atoms. In the second geometry, the oxygen atoms have acquired a negative charge in the singlet state and the charge transfer to the oxygen atoms increases in the higher spin states. The spin densities in this geometry reside almost exclusively on the copper ions. In the fourth geometry wherein the oxygen atoms are not symmetrically placed with respect to the copper ions, the spin density resides almost exclusively on the oxygen atom further away from the copper atoms while the oxygen nearest to the copper ions has the largest charge density.

The small singlet–triplet energy gap in these systems is consistent with the fact that there is only a small rearrangement of charge from the singlet to the triplet state. The large singlet–quintet energy gap indicates a rather large charge density redistribution in the quintet state relative to the singlet state. Stronger exchange integral favours the high-spin ground state and there is a balance between the gain in kinetic energy that is possible in a low-spin state due to large number of path-ways for delocalization and the lower electron repulsion energy in the high-spin state due to larger exchange integral. In the fourth geometry where only one of the oxygen atoms is effectively involved in delocalizing the electron density, the kinetic stabilization of the singlet state relative to the triplet state is only marginal

Table 9. A comparison of ΔE_{ST} ($2J$) and charges in $[Cu_2O_2]^{+2}$ between the two different structures II and III

	Structure II		Structure III	
	Our work	Maddaluno and Giessner-Prettre [20]	Our work	Maddaluno and Giessner-Prettre [20]
ΔE_{ST} (cm^{-1})	1540	1263	726	482
Charge on each oxygen	− 1.16	− 0.34[a]	− 0.23	− 0.60
Charge on each copper	1.16	0.34[a]	0.23	0.60

[a] From the best calculation using ROHF-(GVR) + CI using closed shell for singlet (HONDA)

and the lower electron repulsion in the triplet state leads to a triplet ground state. There is very little net transfer charge between the oxygen atoms and the copper ions while the lower oxygen atom has acquired a net negative charge and the upper oxygen atom has acquired a net positive charge. It is also interesting to note that spin density in the triplet state resides almost exclusively on the upper oxygen atom. At this point it is necessary to compare the results of Maddaluno and Giessner-Prettre [20] with ours at least on two points – the value for singlet–triplet separation and charge densities on oxygen and copper, both being good indications of the properties of hemocyanin. This comparison in the absence of histidine is being considered on the assumption of the earlier workers [17, 20] that the neglect of metal–ligand bonds should hopefully not imply major qualitative differences for the results obtained in X-ray EXAFS and ligand field splitting. It is fortuitous that both their calculations and ours indicate the importance of structures II (called by Maddaluno and Giessner-Prettre as *cis* in Table 1) and III (called by them as *trans* in the same reference). Among them, there is concurrence in the results for II being an acceptable model for $[Cu_2O_2]^{+2}$. This is borne by a comparison of the results from ours and that of Maddaluno and Giessner-Prettre [20] in Table 9.

While comparing our results with theirs we have taken their last results from ROHF-(GVB) + CI(HONDO). Structure II is a proper model for $[Cu_2O_2]^{+2}$ than structure III since (i) both types of calculations predict a singlet ground state for II in accordance to the experimental point of view with triplet being 1540 cm^{-1} above the singlet in our work compared with 1263 cm^{-1} in the work of Maddaluno and Giessner-Prettre [20]; these values being closer to the experimental suggestion of a lower limit of 550 cm^{-1}; this prediction is also better than that of Solomon and coworkers [17]; however, structure III gives a lower magnitude of the gap (726 cm^{-1}) in our prediction while Maddaluno and Giessner-Prettre [20] predict a triplet ground state for this model; (ii) for structure II, our results predict a near transfer of one electron from each copper to oxygen while their results predict a transfer of only 0.34 electron; for structure III, however, our calculation indicates a much smaller transfer of charge from copper to oxygen while their work fares better. Taking all factors into considerations, structure II is probably the best model for $[Cu_2O_2]^{+2}$ if ligands are not to be seriously considered. A comparison on ΔE_{ST}, charge density and spin-density distribution for all models resulting from our calculations are given in Fig. 2.

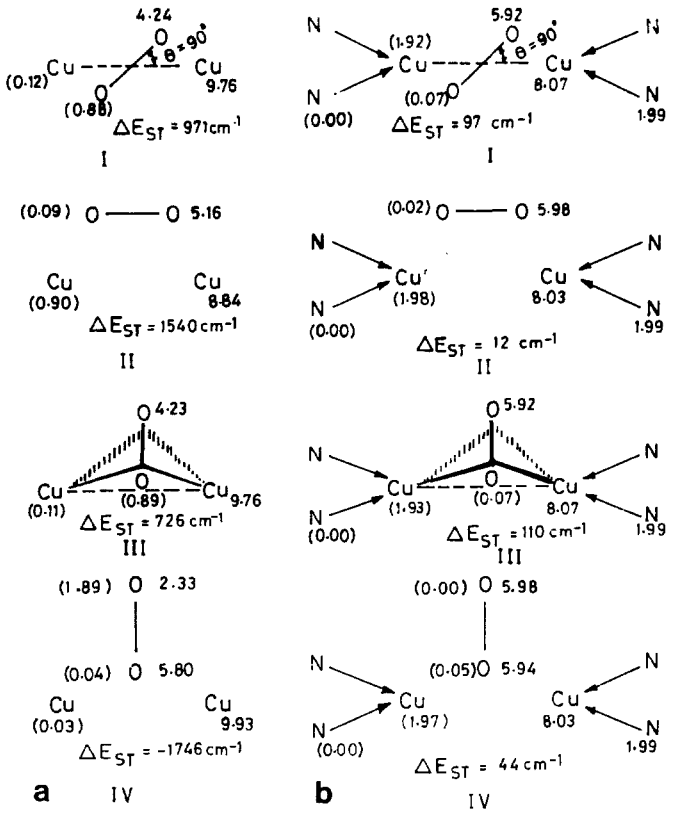

Fig. 2a. Charge densities for singlet and spin-densities (in parenthesis) for triplet and singlet–triplet energy gaps (ΔE_{ST}) for $K(= K_p = K_d) = 0.04$ eV in various models for an active site of hemocyanin as calculated by Diagrammatic Valence Bond approach; **b** Charge densities and spin densities (in parenthesis) in quintet for $K (= K_p = K_d) = 0.02$ eV and singlet–triplet energy gaps (ΔE_{ST}) for $K_p = 0.02$ eV and $K_d = 0.04$ eV in various models for an active site of hemocyanin as calculated by the Diagrammatic Valence Bond approach

3.2 $[Cu_2O_2N_4]^{+2}$ *system*

In the actual oxyhemocyanin system, since the copper atoms are also ligated to nitrogens, for a more realistic understanding of the electronic structure, it is necessary to include the nitrogen atoms also in the calculations. Furthermore, a recent work of Chandler and Manoharan [21] indicates the importance of introducing ligands into $[Cu_2O_2]^{+2}$ with the use of local density functional approach. The geometries we have considered are once again very similar to the systems we have already discussed. The four nitrogen atoms and the copper atoms are in the same plane and the oxygen molecule is placed in four different configurations as shown in Fig. 1.

In Table 10 is shown the energies of the two low-lying states in each spin state for each of the four geometries. For small values of K_p and K_d, the ground state is a singlet in the first and the third geometries and a quintet in the second and fourth geometry. All the excitation gaps in the system are rather small, about 0.05 eV, for

Table 10. Energies in units of cm^{-1} of low-lying states in the four different geometries for the $(Cu_2O_2N_4)^{+2}$ system for different values of the exchange integral K ($= K_p = K_d$) in eV. All the energies are referred to the lowest singlet state for the specified geometry and K. Negative energies imply the state to be more stable than the lowest singlet state

Geometry	Spin states	K (eV)		
		0.02	0.04	0.10
I	S_1	0	0	0
	S_2	438	445	130
	T_1	61	101	− 8
	T_2	382	428	225
	Q_1	1299	315	− 1445
	Q_2	1302	581	− 1443
II	S_1	0	0	0
	S_2	1045	1053	1054
	T_1	14	17	− 4
	T_2	297	619	1072
	Q_1	− 569	− 1185	− 3047
	Q_2	468	− 160	− 2018
III	S_1	0	0	0
	S_2	376	333	302
	T_1	72	101	246
	T_2	350	495	403
	Q_1	919	245	− 1596
	Q_2	1152	479	− 1359
IV	S_1	0	0	0
	S_2	619	621	632
	T_1	36	36	22
	T_2	293	601	638
	Q_1	− 519	− 1141	− 3029
	Q_2	23	599	− 2488

the states for which we have calculated the energies. Increasing the direct exchange integral beyond ≈ 0.1 eV leads to a quintet ground state in all the geometries. It is observed that with unequal values for the exchange integrals K_p and K_d, the quintet state is more sensitive to K_d than K_p, in all the geometries (Table 11).

The charge density data (Table 12) shows very interesting changes from the system having no nitrogen atoms ($[Cu_2O_2]^{+2}$). In all the states, as well as in all the geometries, the oxygen atoms are in a nearly closed shell configuration with two electrons transferred from each of the copper atoms. The nitrogen orbital is also nearly doubly occupied. Even in the fourth geometry where the oxygens are not symmetrically placed, the charge transfer to the two oxygen atoms is nearly complete leading to an almost complete p shell. The spin densities reside almost exclusively on the copper sites as seen in the case of the quintet states. The triplet spin densities are more difficult to obtain in this case as the eigenfunction accuracy has to be much greater due to the small energy gaps between the triplet states. However, the charge density data clearly indicates that even in the triplet states

Table 11. Energy levels in units of cm^{-1} for different spin subspaces in $[Cu_2O_2N_4]^{+2}$ for various values of $K_p \neq K_d$. All the energies are referred to the lowest singlet state for the specified geometry and K. Negative energies imply the state to be more stable than the lowest singlet state

Geometry	Spin	K_p, K_d (eV)			
		0.04, 0.02	0.02, 0.04	0.10, 0.02	0.02, 0.10
I	S_1	0	0	0	0
	T_1	36	97	60	− 23948
	Q_1	932	616	859	− 25173
II	S_1	0	0	0	0
	T_1	61	12	8	18
	Q_1	− 576	− 579	− 581	− 3019
III	S_1	0	0	0	0
	T_1	65	110	64	261
	Q_1	888	279	300	− 1459
IV	S_1	0	0	0	0
	T_1	34	44	36	40
	Q_1	− 532	− 1135	− 531	− 2990

Table 12. Charge and spin densities in quintet for $[Cu_2O_2N_4]^{+2}$ for $K\,(= K_p = K_d) = 0.02$ and 0.04 eV. O^U and O^L refer to upper and lower oxygen atoms in geometry IV

Geometry	Atoms	K (eV)			
		Charge density		Spin density	
		0.02	0.04	0.02	0.04
I	Cu	8.070	8.060	1.924	1.922
	O	5.920	5.920	0.072	0.075
	N	1.990	1.990	0.004	0.004
II	Cu	8.030	8.030	1.980	1.981
	O	5.980	5.980	0.017	0.018
	N	1.990	1.990	0.001	0.001
III	Cu	8.070	8.050	1.929	1.927
	O	5.920	5.930	0.066	0.066
	N	1.990	1.990	0.004	0.004
IV	Cu	8.030	8.020	1.968	1.971
	O	5.980	5.990	0.000	0.000
	O	5.940	5.940	0.051	0.051
	N	1.990	1.990	0.003	0.001

the spins reside on the copper sites. Another interesting point to note is that the high-spin state eigenvalues are more sensitive to the direct exchange integral on the copper atoms rather than on the oxygen atoms. Thus we see from Table 11 that the stability of the high spin states is greater when K_d is large and K_p is small. The stability is greatly reduced when the K_d and K_p values are interchanged.

We note that in this system, the phase space available for the delocalization of the electrons has increased by the introduction of the nitrogen lone pairs. To exploit the increased phase space and to reduce kinetic energy of the system, it is essential that the copper atoms have partly filled orbitals. This indeed is the case is seen from the charge densities wherein we find extensive charge transfer from the copper atoms to the oxygen atoms in all the geometries including geometry IV. It is for this reason that the energies are more sensitive to the direct exchange integral K_d of the copper atom compared to K_p on the oxygen atom. All the energy gaps in the system are also rather small compared to the previous system as the different spin states can be obtained by flipping the spins without changing the charge density distribution.

If the oxyhemocyanin system is found to be of singlet ground state, then we can rule out the fourth geometry. Our studies with the nitrogen atoms also rule out the second geometry in which the oxygen molecule is placed horizontally above the $[Cu_2N_4]$ plane since the quintet state becomes the ground state making ΔE_{ST} experimentally meaningless. The only two possible geometries are then the first and the third. In both these geometries, the oxygen molecule is placed perpendicular to the Cu–Cu bond. In the first geometry, all the atoms are in the same plane while in the third geometry, the oxygen molecule lies above the Cu–N plane. In both the first and the third geometry, the energy gaps, the charge densities and the spin densities are very similar and it is unlikely that just the energy gap and spin density measurements can distinguish between these two possibilities. However, on the basis of the results from $[Cu_2O_2]^{+2}$ and $[Cu_2O_2N_4]^{+2}$ we can probably point out that geometry III is a better model. It is still not understood why the introduction of nitrogen ligands have pushed the electronic charges from copper to oxygen so drastically (see Fig. 2) to make copper almost Cu^{3+}. It is therefore, possible to mention that structure II is favourable for $[Cu_2O_2]^{+2}$ and structure III for $[Cu_2O_2N_4]^{+2}$. The part played by the ligand is to be critically looked into.

4 Summary and conclusion

We have carried out full CI calculations on the $[Cu_2O_2]^{+2}$ and $[Cu_2O_2N_4]^{+2}$ systems taking into account the five $3d$ orbitals of coppers, the three $2p$ orbitals of the oxygens and the σ bonding lone pair orbitals of the nitrogen atoms directed towards the copper atoms. We have employed a model Hamiltonian which includes all possible transfer integrals amongst these orbitals in a consistent manner. The Hamiltonian also includes electron repulsion integrals corresponding to repulsions between (i) two electrons within the same orbital, (ii) an electron in each one of a pair of orbitals within the degenerate manifolds of a given atom and (iii) electron repulsions between an electron in a given orbital on one atom and an electron in another orbital of another atom parameterized using Ohno interpolation scheme [27]. We also include the two-electron exchange integral between degenerate orbitals on a given atom.

We find that the spin of the ground state depends upon the geometry as well as the direct exchange constants K_d and K_p. For small values of the exchange constant, in two geometries the ground state is a singlet and in the other two the ground state is a high-spin state. For large direct exchange constant, the ground state switches over to a quintet state in all the cases. The geometries in which the ground state is a singlet are closely related and correspond to the O–O bond being perpendicularly placed with respect to the Cu–Cu axis. The lowest excited triplet is

at an energy of 110 cm^{-1} and there is extensive charge transfer between the copper atoms to the oxygen atoms leading to an almost completely filled $2p$ shell on the latter. However, the geometry II seems to fit into the picture if one considers only the $[Cu_2O_2]^{+2}$ as the real active site. The spin density in the high-spin states are almost exclusively found on the copper atoms, consistent with the charge density distribution. Thus, if the oxyhemocyanin system is in the singlet ground state with a small singlet–triplet energy gap, the possible geometries predicted by our calculations are the perpendicular geometries III if we consider with respect to Table 11 ($K_p = \frac{1}{2}K_d$) $[Cu_2O_2N_4]^{+2}$ and II for $[Cu_2O_2]^{+2}$ as active sites.

Acknowledgements. We are thankful to the Jawaharlal Nehru Center of Advance Scientific Research for computing facility. One of us (PKM) thanks the CSIR for fellowship. Financial assistance from the project (SP/S1/F-47/90) by the Department of Science and Technology. Govt. of India is acknowledged.

References

1. Fernandez-Moran H, Van Bruggen EFJ (1966) J Molec Biol 16:191
2. Mellema JE, Klug A (1972) Nature 239:146
3. Van Holde KE (1982) Rev Biophys 15:1
4. Holde KE, Bruggen EF (1971) In: Timasheff SN, Fasman GD (eds) Subunits in Biological Systems:Part A. Marcel Dekker, New York, pp 1–53
5. Dooley DM, Scott RA, Ellinghaus J, Solomon EI, Gray HB (1978) Proc Nat Aca Sci USA 75:3019
6. Larrabee JA, Spiro TG (1980) J Am Chem Soc 102:4217 and references therein
7. Eickman NC, Himmelwright RS, Solomon EI (1979) Proc Nat Aca Sci USA 76:2094
8. Himmelwright RS, Eickman NC, Solomon EI (1979) J Am Chem Soc 101:1576
9. Hodgson MS, Eccles KO, Lontie R (1981) J Am Chem Soc 103:984
10. Anne Volbeda, Hol WGJ (1989) J Mol Biol 209:249
11. Hazes B, Magnus KA, Bonaventura C, Bonaventura J, Dauter Z, Kalk KH, Hol WGJ (1993) Protein Science 2:597
12. (a) Karlin KD, Cruse RW, Gultneh Y, Hayes JC, Zubieta J (1984) J Am Chem Soc 106:3372. (b) Karlin KD, Cruse RW, Gultnech Farooq A, Hayes JC, Zubieta J (1987) J Am Chem Soc 109:2668
13. Kitajima N, Koda T, Mora-oka Y, Toriumi K (1989) J Am Chem Soc 111:8975
14. Kitajima N, Koda T, Hashimoto S, Kitawaga T, Mora-oka Y (1990) J Am Chem Soc 1 12:8833
15. Fenton DE, Lintvedt RL (1978) J Am Chem Soc 100:6357
16. Fenton DE (1989) Pure Appl Chem 61:903
17. Ross PK, Solomon EI (1990) J Am Chem Soc 112:5871
18. Ross PK, Solomon EI (1991) J Am Chem Soc 113:3246
19. Baldwin MJ, Ross PK, Pate JE, Tyeklar Z, Karlin KD, Solomon EI (1991) J Am Chem Soc 113:8671
20. Maddaluno J, Giessner-Prettre C (1991) Inorg Chem 30:3439
21. Chandler CS, Manoharan PT (1993) Proc XXIX ICCC, University of Lussane, Switzerland and results to be communicated
22. Pravat K Mandal, Bhabadyuti Sinha, Manoharam PT, Ramasesha S (1992) Chem Phys Letters 191:448
23. Pravat K Mandal, Manoharan PT (1993) Chem Phys Letters 210:463
24. Zhang FC, Rice TM (1988) Phys Rev B 37:3759
25. Hybertsen MS, Schlulet M (1989) Phys Rev B 39:9028
26. Ramasesha S, Rao CNR (1991) Phys Rev B 44:7064
27. Ohno K (1964) Theor Chim Acta 2:219

28. (a) Pople JA, Santry DP, Segal GA (1965) J Chem Phys 43:1965. (b) Pople JA, Beveridge D (1970) Approximate Molecular Orbital Theory. McGraw-Hill, New York
29. (a) Pariser R, Parr RG (1953) J Chem Phys 21:466. (b) Klein DJ, Soos ZG (1971) Mol Phys 20:1013
30. Bhabadyuti Sinha, Ramasesha S (1993) Phys Rev B 48:16410
31. Soos ZG, Ramasesha S (1990) In: Valence Bond Theory and Chemical Structure. Klein DJ, N Trinajstich (ed) Elsevier, Amsterdam
32. Ramasesha S, Albert IDL, Bhabadyuti Sinha (1991) Mol Phys 72:537
33. Rettrup S (1982) J Comput Phys 45:100
34. (a) Hubbard J (1963) Proc Roy Soc Lond Ser A 276:238. (b) ibid (1964) 277:237. (c) ibid (1964) 281:401
35. Kanamori J (1963) Prog Theor Phys 30:275
36. Gutzwiller MC (1963) Phys Rev Lett 10:159